

SEPIC Converter Based Maximum Power Point Tracking of a Photovoltaic System Using State-Space Feedback Controller

Ahmad Moghassem¹, Nader Javadifar^{2*}

Abstract – In this paper, an intelligent control system using state-space feedback controller designed to track the maximum power radiation direction of the sun for a photovoltaic system in a varying direction environment will be studied. In fact, the study focuses on the ability of using the state space feedback controller to control the power oscillation around the optimal point such that the power dissipation is minimized. Furthermore, the control system based on the instantaneous power tracking and with respect to the nonlinear photovoltaic cell makes feasible to access the maximum possible electric power using tiny changes in the Single Ended Primary Inductor Converter (SEPIC).

Keywords: Photovoltaic, Single Ended Primary Inductor Converter, Maximum Power Tracking

1. Introduction

Nowadays, closing to the end of the fossil fuel ages and increasing concerns about negative effects of them on the environments, have caused to boost up usage of the renewal energies significantly. Total installed capacities of renewal energies, in general and electricity, in specific, have experienced a notable growth through the years 2008 to 2018. In this period, capacity of the photovoltaic (PV) energy resources installed has a mean annually growth of 60%, which is the fastest growth among all the energy resources. One of the attractive features of PV systems is their capability to be implemented in small scales. Using the electric power production in local points near the end customers, the transmission power loss can be brought to zero.

The efficiency of the PV systems, technically, is dependent upon the sun radiation onto the solar cells, quality and type of the PV cells, the temperature of the cells, connections between cell modules, adaptive impedance between modules, DC/DC converters and types of adopted converters [1].

During the last years, there have been numerous tracking methods for the maximum power direction [2], typically more than 30 ones [3-10]. These methods differ from each other based on the complexity of sensors requirements, speed of tracking, cost, practical efforts and capability to track the maximum local powers [2]. On the other hand, some methods such as fuzzy systems and neural

networks have shown to possess more accuracy and speed, although they come at the cost of more complexities. The fuzzy systems based methods are highly dependent on the user experience in designing the fuzzy rules, while neural networks need unique as well as repetitive trainings [11-12]. The enhanced tuning method has been considered as one of the best Maximum Power Point Tracking (MPPT) [13-14] in most of the solar systems due to their simple set-up, high accuracy and speed, great reliability and capability to work in variable atmospheric environments. The common approaches of MPPT are usually comprised of two individual control loops; the first of which includes MPPT that produces an error signal which becomes zero when power is at its maximum point. The aim of the second loop is taking the error signal close to zero [5]. The PI controllers are widely acceptable in linear control systems due to their simplicity of set-up and design, and low maintenance costs. These system runs in two modes: voltage and current. Nevertheless, since the solar arrays are intrinsically nonlinear and the environment in which systems must to operate is unpredictable, MPPT becomes a nonlinear problem in solar systems renewal energy and thus, the PI controllers does not give rise to acceptable results [15].

2. Problem Formulation

The block diagram of the solar electric power generation has been shown in Fig. 1 and the schematic diagram of the MPPT in Fig. 2, where the MPPT is made up of three sections: the photovoltaic cells, the SEPIC converter and power consumer load. In the followings, each of these sections will be modeled.

2* Corresponding Author- Department of Electrical Engineering , Aliabad Katoul Branch, Islamic Azad University, Aliabad Katoul ,Iran

Email: javadifar@aliabadiau.ac.ir

1- Department of Electrical Engineering , Damghan Branch, Islamic Azad University, Damghan ,Iran

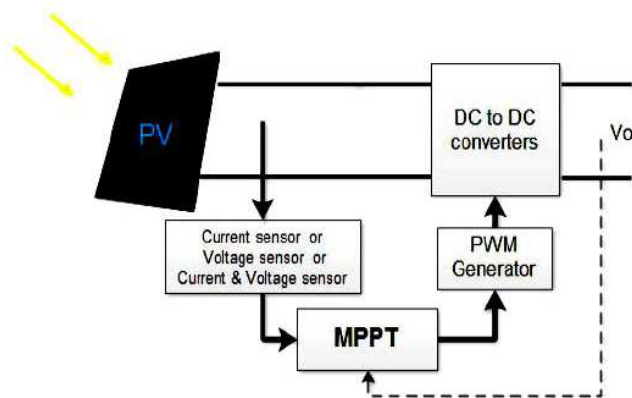


Fig. 1: The block diagram of the solar electric power generation system

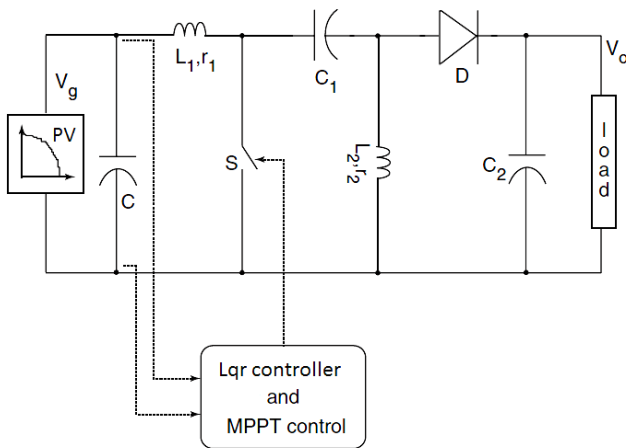


Fig. 2: The schematic diagram of the MPPT and the corresponding controller

2.1. Equivalent Electrical Circuit of the Solar Cell

The photovoltaic (PV) cells are made up of P-N bonds fabricated on layers of semiconductors. Therefore, a solar cell while in the state of generating electric power and connected to an electrical load, can be modeled electrically as in Fig. 3, i.e., an electrical circuit comprising a current source paralleled with a diode. In practice, when the model includes necessary connections of PV, a serial resistance R_s and a paralleled one R_{sh} are added to the circuit. These resistors are to represent the power loss of the cell. The power loss are caused by factors such as reflection of the sun beam from the cell surface, absorbing photons without creation of any electrons, the free holes and recombination of the electrons with free holes [15-16].

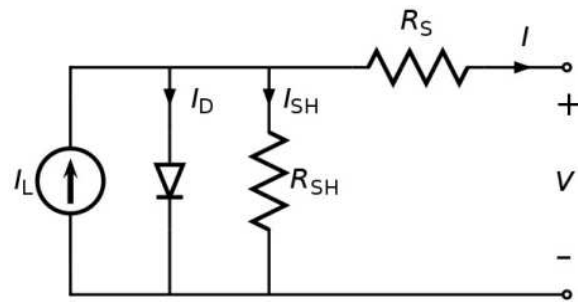


Fig. 3: The equivalent electrical circuit of a solar cell

The electrical source representing the power generated by the solar cell can be shown as:

$$I = I_L - I_0 \left(E^{\frac{q(V+IR_s)}{nkT}} - 1 \right) - \frac{V+IR_s}{R_{sh}} \tag{1}$$

in which, I_L is the current generated by the sun radiations, I_0 , the inverse saturation or the leakage current of the diode, q , the electric charge of an electron ($1.60217646 \times 10^{-19}$ C), K , the Boltzmann constant ($1.3806503 \times 10^{-23}$ J/K), T , the temperature of the P-N bond in Kelvin degree and n , the ideal diode constant.

The electrical efficiency of the PV, during the practical operation, is decreased by the internal resistances including connections as well as the leakage currents on either side of the section. These parasite resistances, as shown in Fig. 3, can be modeled using serial and parallel resistor (R_s and R_{sh}). In an ideal cell, R_{sh} is infinite, showing absence of any leakage route for current, and R_s is zero, representing lack of any element for voltage drop before the load. As it can be seen in Fig. 4, when R_{sh} decreases, value of V_{OC} drops; while in a similar fashion increasing R_s decreases the I_{SC} . Altogether, decreasing either the parallel resistor or increasing the serial one will be resulted in reduction of efficiency [13-14].

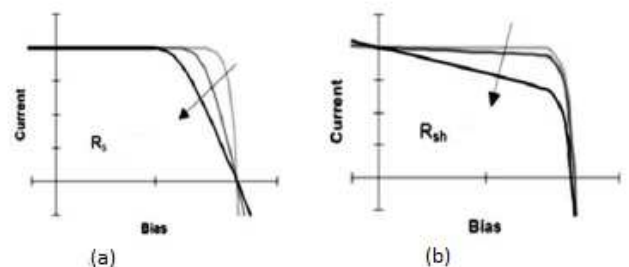


Fig. 4: Effect of variation of resistors on the current characteristics. (a) R_s increase , (b) R_{sh} decrease

2.2. Modeling SEPIC Converter

There are a variety of DC-DC boost up converters options to increase the lower voltage to higher values; however, the available designs suffer from the high enough efficiency. Among these converters, one is SEPIC, which is illustrated in Fig. 5. SEPIC operates in two modes as follows.

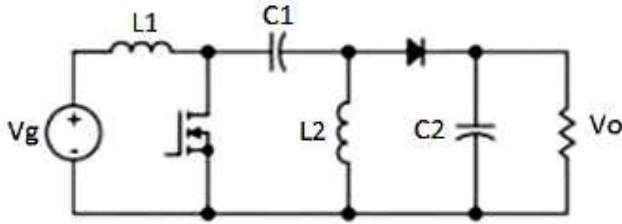


Fig. 5: SEPIC converter circuit

• First Operation Mode

When the switch is on, L1 inductor will be charged and L2 receive its energy through the capacitor C1. During this time, C2 is used to supply the output load and no power is transmitted from the input. Fig. 6 shows SEPIC while operating in this mode.

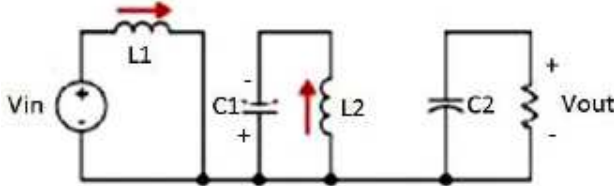


Fig. 6: First mode of SEPIC operation

• Second Operation Mode

In this case, the switch is off and both inductors supply C2 simultaneously. The inductor L1 would charge the capacitor C1 during this time interval. Fig. 7 demonstrates the circuit operation in the second mode.

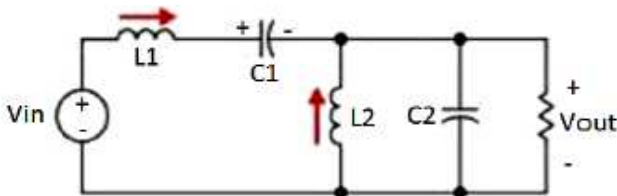


Fig. 7: Second mode of SEPIC operation

In order to derive the state space model of SEPIC such that it represents the two operation modes, the conditions of the Table 1 must be taken into account.

Table.1: Different operation modes of SEPIC

State 1	Switch on	Diode off
State 2	Switch off	Diode on

Following the above conditions, then the state space model of SEPIC will be derives as:

$$\dot{X} = AX + BU \tag{2}$$

where

$$A = A_1 D_1 + A_2 D_2$$

$$B = B_1 D_1 + B_2 D_2$$

$$D_1 + D_2 = 1$$

(3)

and the matrices A and B are defined as:

$$A = \begin{bmatrix} -\frac{r_1}{L_1} & 0 & -\frac{D_2}{L_1} & -\frac{D_2}{L_1} \\ 0 & -\frac{r_2}{L_2} & -\frac{D_1}{L_2} & -\frac{D_1}{L_2} \\ \frac{D_2}{C_1} & -\frac{D_1}{C_1} & 0 & 0 \\ \frac{D_2}{C_2} & \frac{D_2}{C_2} & 0 & -\frac{1}{RC_2} \end{bmatrix} \tag{4}$$

$$B = \begin{bmatrix} \frac{1}{L_1} \\ 0 \\ 0 \\ 0 \end{bmatrix} \quad X = \begin{bmatrix} i_1 \\ i_2 \\ vc_1 \\ vc_2 \end{bmatrix} \quad U = [V_A] \tag{5}$$

Then, the permanent voltage gain is obtained using the relationship :

$$X_{ss} = -A^{-1}BU \tag{6}$$

$$\frac{V_0}{V_A} = \frac{RD_1 D_2 (D_1 + D_2)}{\left\{ RD_2^2 (D_1 + D_2)^2 + (r_1 D_1^2 + r_2 D_2^2) \right\}} \tag{7}$$

If we consider $D_1=D_2$ and $V_1=V_2$ and $r \ll R$, the relationship between the voltage of solar cells array and that of the load will be as in equation (8):

$$V_o = \frac{V_A D}{(1 - D)} \tag{8}$$

3. The Proposed Method

As we mentioned, the purpose of the study is tracking the maximum power point when the any increase decrease of the load connected to the solar cell would result in increased ad decreased power consumption, too. In fact, variation of the load causes change in the slope of the linearized resistor, and thus, the optimal operating point. This problem can be overcome using the SEPIC converter and LQR control for handling the on-state in a switching period (D). Of course, the switching period (D) changes as the time or state of the cell changes in a way such that the optimal operation point is achieved and maximum power is delivered to the load.

The PV system is optimal gives the maximum efficiency when in any occasion, the generated power of the solar panel is maximized, i.e. it operates at the MPP point. Using changes in switching period duration, the characteristic load from the solar cell viewpoint will changes from zero to infinity. The characteristic curve of the solar cell output power versus D variations are depicted in Fig. 8 and 9.

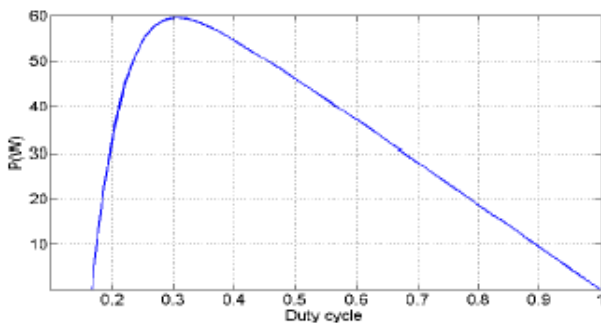


Fig. 8: Variations of the output power of the solar cell versus variation of D

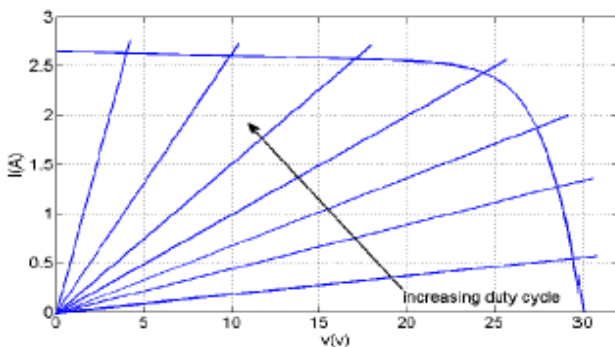


Fig. 9: Characteristic curves of the solar cell and that of the load versus the variation of D

One the suitable methods to track the maximum power point, is the squared voltage which is, in comparison of taking feedback of the current, both lower costly and simpler. The current sensors, due to their large ripple in various environments need tuning as well as controlling circuits, which make them more difficult to be accessible. In power maximization based on the squared load voltage, the adopted power electronic converter will be considered as a variable resistor in PV cells, their power would be a function of squared voltage and variable load resistor, and both are functions of the duty cycle of this converter. In fact, in this method, relationship of generated power of the PV source would be $P_g = kVA$, in which:

$$k = \frac{1}{R_{eq}} \tag{9}$$

In this paper, in order to access the maximum power of the PV cell, the state space feedback controllers are employed. These controller, against the classical controllers are considered as modern controllers. In modern control, for the system under study, the state equations will be used for the analysis of stability, controllability and observability, without transferring the system equations into the frequency domain; in this case, the state feedback is used for the purpose of the system control. Among the advantage of this method are simplicity of the analysis and implementation, and most importantly, optimization capability of a cost function (or the objective function) even in the presence of system control.

4. LQR Controller Design

The optimal control of the LQR state feedback is defined as follows:

Consider a LTI system with given initial conditions,

$$\dot{x} = Ax + Bu \tag{10}$$

Then we are interested in designing the control of the state feedback $u = -kx$ such that it minimizes the following function,

$$J = \int_0^{\infty} [x^T Qx + u^T Ru] dt \tag{11}$$

In (11), the matrices Q and R are symmetric and furthermore, we have $R \geq 0$ and $Q \geq 0$. Then the closed loop equation and optimality function of the system would be,

$$\dot{x} = (A - Bk)x$$

$$J = \int_0^{\infty} x^T(t)(Qx + k^T Rk)x(t)dt \tag{12}$$

For this problem to have any solution, first, controller needs to be able to stabilize the system. Therefore, the instable modes should be able to be stabilized or more generally, system should be controllable.

5. Simulation Results

In order to simulate the PV source, we have used a real typical standard ones as given in [17]. The constant parameters of the SEPIC converter and that of solar cell are given in Tables 2 and 3, respectively.

Table 2: Constant parameters of the SEPIC converter

Parameter	quantity
R ₁	0.05
R ₂	0.05
L ₁	5000e-6
L ₂	5000e-6
C ₁	5000e-6
C ₂	5000e-6
C	100e-6
R	20

Table 3: Constant parameters of the solar cell

Parameter	Quantity
Max Power	200
Voltage of Max Power	26.3
Current of Max Power	7.61
Open circuit Voltage	32.9
Short circuit current	8.21

The first parameter to analyze are inductors L1 and L2 in the SEPIC converter. As it can be observed in Figs. 10 and 11, the currents i_1 and i_2 have reached the steady state values and track their references.

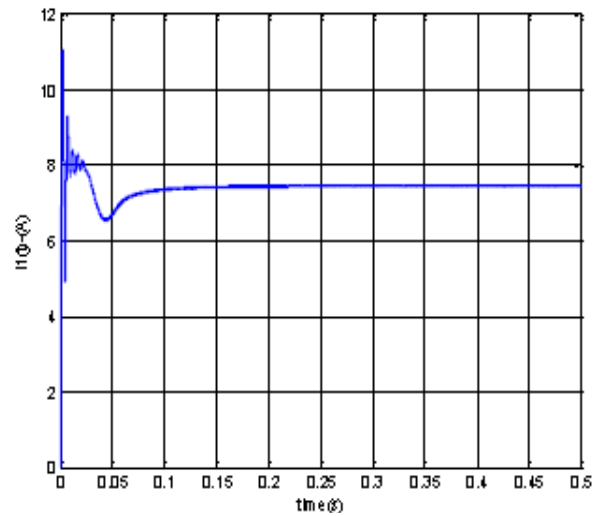


Fig. 10: The instantaneous current of the L1 in SEPIC converter

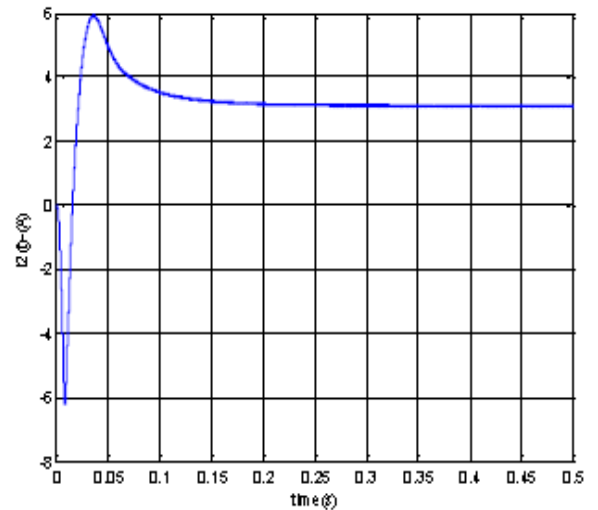


Fig. 11: The instantaneous current of L2 in SEPIC converter

The other parameters to be studied are voltages number one and two in the SEPIC converter. From the Figs. 12 and 13, the voltages V_1 and V_2 have gotten the steady state quickly and follow their references values, respectively.

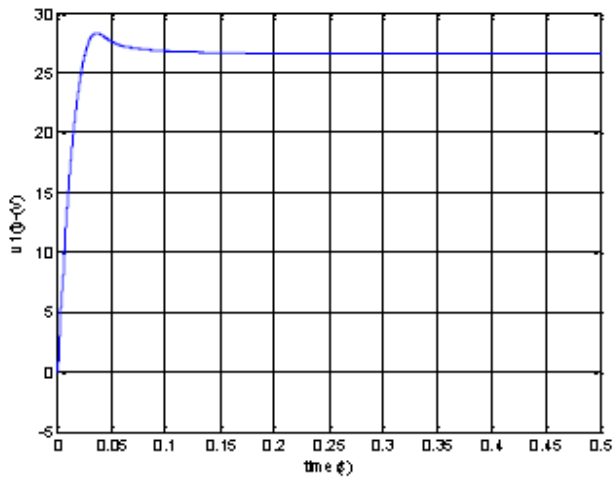


Fig. 12: The instantaneous voltage of C1 in SEPIC converter

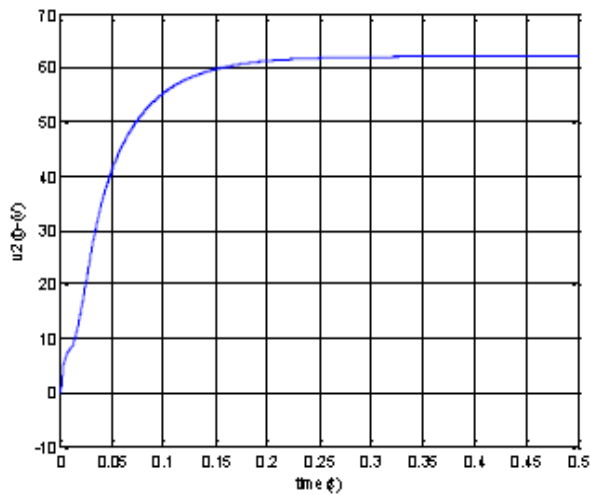


Fig. 13: The instantaneous voltage of C2 in SEPIC converter

Figs. 14 and 15 illustrates variations of output voltage and current of the PV cell and parameters of LQR controller with respect to time. Again, operating are followed by the SEPIC converter and LQR controller exactly and their steady state and final values have been reached within a fraction of time.

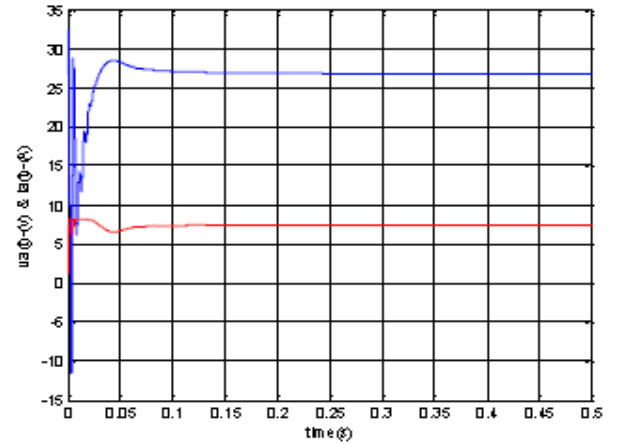


Fig. 14: The variations of voltage and current of PV source versus time

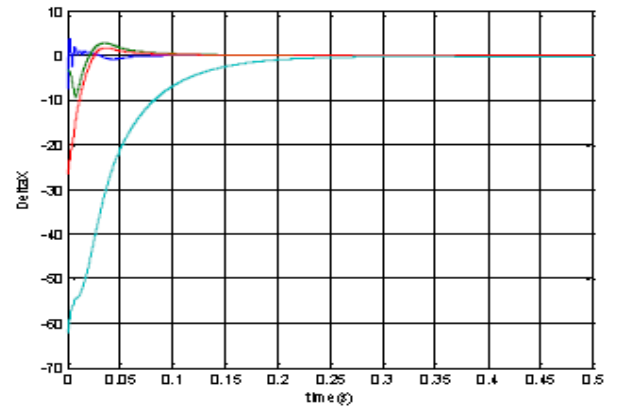


Fig. 15: The variations of LQR's control parameters versus time

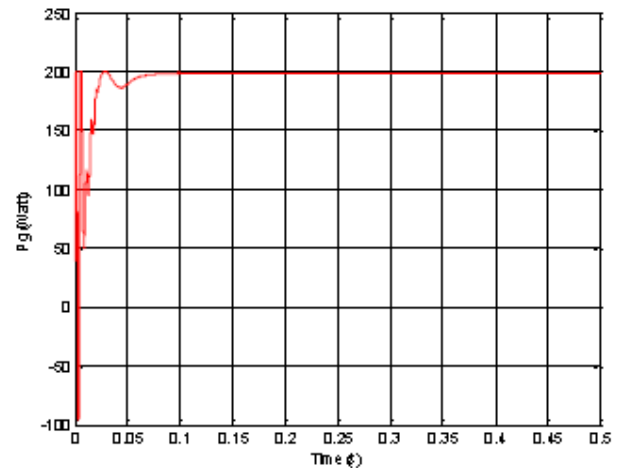


Fig. 16: The variation curve of the PV source's output power

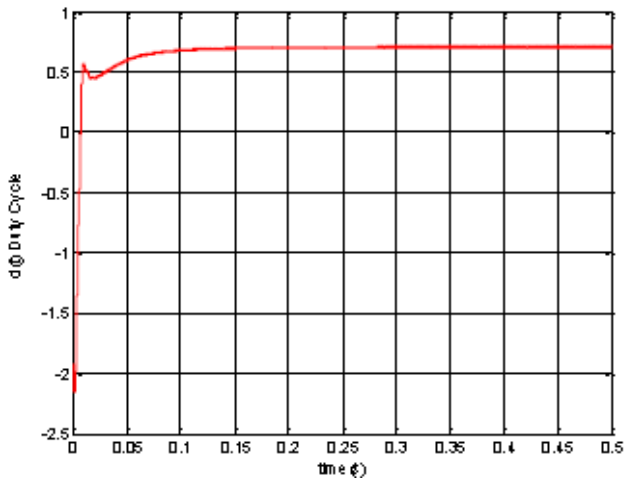


Fig. 17: The variation curve of duty cycles of switching (D)

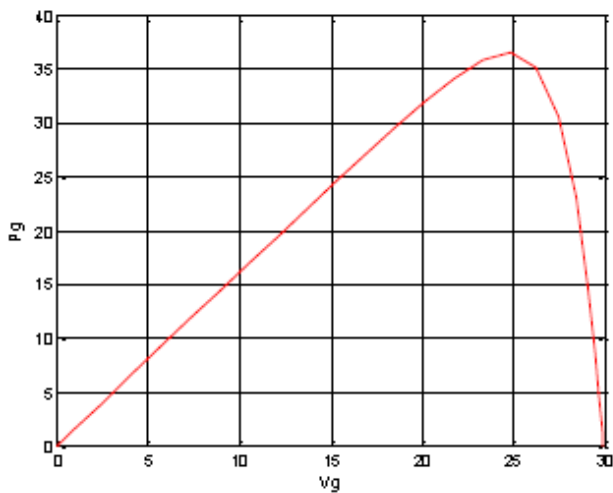


Fig. 18: The variation of PV's output power versus the output voltage

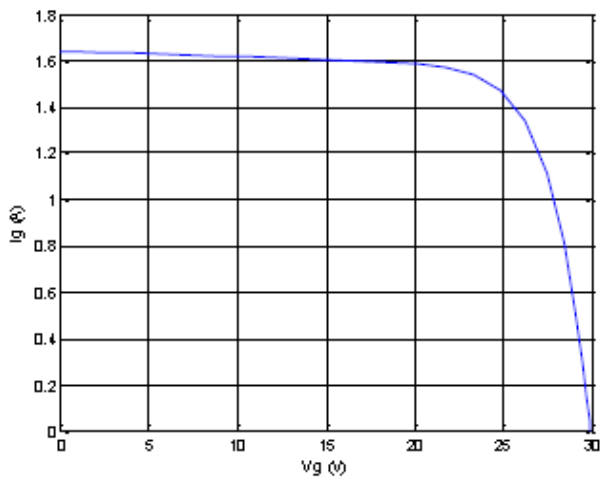


Fig. 19: The variation of the output current versus the output voltage of PV cell

6. Conclusions

Because of the high cost of Photovoltaic (PV) systems and their low efficiencies, these systems must operate at their optimal utilization points. Since these conditions depend on the specific load, the load variations implies usage of a control system that is able to identifies the optimal power points and accordingly follow them. In order to place the solar panels such that the maximum power is generated, there are problems such as nonlinearity of the characteristic curve of the solar cells and also the variability of this curve against the sun radiation and changes in output loads. In this paper, we have shown that these challenges can be overcome using LQR controllers and SEPIC converters.

References

- [1] Sebastijan Seme, Gorazd Štumberger, Jožec Voršič. APRIL, Maximum Efficiency Trajectories of a Two-Axis Sun Tracking System Determined Considering Tracking System Consumption. IEEE TRANSACTIONS ON POWER ELECTRONICS, 2011, Vol:26, No. 4, 1280 – 1290
- [2] Q.Me, M.Shan, L.Liu, J.M.Guerrero, "A Novel Improved Variable Step-Size Incremental Resistance (INR) MPPT Method for PV Systems," IEEE Trans. Ind. Electron., vol. 58, no. 6, pp. 2427–2434, Jul. 2008.
- [3] V.Agarwal, A.Vishwakarma, "A Comparative Study of PWM Schemes for Grid Connected PV Cell," Power Electronics and Drive Systems. PEDS '07. 7th International Conference, pp.1769 – 1775,2007.
- [4] M.Berrera, A.Dolara, R.Faranda, S.Leva, "Experimental test of seven widely-adopted MPPT algorithm," IEEE Bucharest Power Tech Conference, pp. 1 – 8,2009.
- [5] T.Esram, P.L.Chapman, "Comparison of Photovoltaic Array Maximum Power Point Tracking Techniques," IEEE transactions on energy conversion, vol. 22, no. 2, june 2007.
- [6]Rakhshan, Mohsen, et al., "Maximum power point tracking control of photovoltaic systems: A polynomial fuzzy model-based approach." IEEE Journal of Emerging and Selected Topics in Power Electronics 6.1 (2017): 292-299.
- [7] Goud, J. Saikrishna, R. Kalpana, and Bhim Singh, "A hybrid global maximum power point tracking technique with fast convergence speed for partial-shaded PV systems." IEEE Transactions on Industry Applications 54.5 (2018): 5367-5376.
- [8] Aquib, Mohd, Sachin Jain, and Vivek Agarwal, "A time-based global maximum power point tracking

technique for PV system." IEEE Transactions on Power Electronics 35.1 (2019): 393-402.

[9] Yousri, Dalia, et al., "A novel chaotic flower pollination algorithm for global maximum power point tracking for photovoltaic system under partial shading conditions." IEEE Access 7 (2019): 121432-121445.

[10] Sangwongwanich, Ariya, and FredeBlaabjerg, "Mitigation of interharmonics in PV systems with maximum power point tracking modification." IEEE Transactions on Power Electronics 34.9 (2019): 8279-8282.

[11] J.L.Agorreta, L.Reinaldos, R.Gonzalez, M.Borrega, J.Balda, L.Marroyo, "Fuzzy switching technique applied to PWM boost converter operating in mixed conduction mode for PV systems," IEEE Trans. Ind. Electron., vol. 56, no. 11, pp. 4363–4373, Nov. 2009.

[12] A.Varnham, A.M.Varnham, G.S.Virk, D.Azzi, "Soft computing model based controllers for increased photovoltaic plant efficiencies," IEEE Trans. Energy Convers., vol. 22, no. 4, pp. 873–880, Dec. 2007.

[13] A. Safari, S. Mekhilef, "Simulation and Hardware Implementation of Incremental Conductance MPPT With Direct Control Method Using Cuk Converter ", IEEE Trans. Ind. Electron., vol. 58, no. 4, pp. 1154– 1161, APRIL 2011.

[14] F.Salem, M.S.Adel Moteleb, H.T.Dorrah, "An enhanced fuzzy PI controller applied to the MPPT problem," J. Sci. Eng., vol. 8, no. 2, pp.147–153, 2005.

[15] Basim Alsayid and Jafar Jallad. 2011. Modeling and Simulation of Photovoltaic Cells/Modules/ Arrays. International Journal of Research and Reviews in Computer Science(IJRRCS).Vol.2.No.6. ISSN:2079-2557

[16] A. Blorfan, D. Flieller, P. Wira, G. Sturtzer, J. Merckle. October 2010. A New Approach for Modelling the Photovoltaic Cell Using Orcad Comparing with the Model Done in Matlab. International Review on Modelling and Simulations (I.R.E.MO.S.), Vol. 3, No. 5 .

[17] High Efficiency Multi-crystal Photovoltaic Module, KC200GT, MODULE : UL1703 certified, FACTORY : ISO9001 and ISO 14001.